Inorg. Chem. **2008**, *47*, 3483−3485

Inorganic Chemistry
Communication

Determination by High-Frequency and -Field EPR of Zero-Field Splitting in Iron(IV) Oxo Complexes: Implications for Intermediates in Nonheme Iron Enzymes

J. Krzystek,[†] Jason England,[‡] Kallol Ray,[‡] Andrew Ozarowski,[†] Dmitry Smirnov,[†] Lawrence Que, Jr.,[*,‡] and Joshua Telser[*,§]

National High Magnetic Field Laboratory (NHMFL), Florida State University, Tallahassee, Florida 32310, Department of Chemistry, University of Minnesota, Minneapolis, Minnesota 55455, and Department of Biological, Chemical and Physical Sciences, Roosevelt University, Chicago, Illinois 60605

Received March 6, 2008

$[Fe^{IV}O]^{2+}$ species have been implicated as the active form of many nonheme iron enzymes. The electronic structures of iron(IV) oxo complexes are thus of great interest. High-frequency and -field electron paramagnetic resonance is employed to determine accurately the spin Hamiltonian parameters of two stable complexes that contain the Fe═O unit: $[FeO(TMC)(CH_3CN)](CF_3SO_3)_2$, where TMC = tetramethylcyclam and $[FeO(N4py)](CF_3SO_3)_2$, where **N4Py** = bis(2-pyridylmethyl)bis(2-pyridyl)methylamine. Both complexes exhibit zero-field splittings that are positive, almost perfectly axial, and of very large magnitude: $D = +26.95(5)$ and $+22.05(5)$ cm^{-1}, respectively. These definitive experimental values can serve as the basis for further computational studies to unravel the electronic structures of such complexes.

High-valent iron(IV) oxo intermediates are likely to be the active species of many mononuclear nonheme iron enzymes that activate dioxygen.[1,2] Within the last 4 years, such species have been identified in several enzymes and characterized as having a high-spin (d^4, $S = 2$) terminal $[Fe^{IV}{=}O]^{2+}$ unit.[3] Within the same time frame, a number of synthetic mononuclear nonheme iron(IV) oxo complexes bearing tetra- and pentadentate N-donor ligands have been reported and characterized by a variety of spectroscopic techniques.[4,5] In contrast to the enzymatic systems, the model complexes generally possess an intermediate-spin, triplet ($S = 1$) ground state,[4,5] which DFT[6] calculations suggest to be less reactive than the corresponding HS, quintet ($S = 2$) state at carrying out H-atom abstractions.[7] Nevertheless, certain synthetic complexes can attack strong C−H bonds such as those of cyclohexane.[8] To rationalize this result, Shaik and co-workers have proposed a TSR model that posits participation of a low-lying $S = 2$ excited state that intersects with the $S = 1$ state along the reaction trajectory.[7]

All synthetic iron(IV) oxo complexes characterized to date have large positive zfs,[9] as given by the axial zfs parameter, $D > +20$ cm^{-1}. This zfs originates primarily from spin–orbit coupling between the ground-state spin triplet and the first excited-state quintet,[10] and its magnitude is inversely proportional to the energy separation between the two. Thus, the magnitude of zfs may assist in quantifying the TSR model by providing the triplet−quintet energy separation. Experimental determination of zfs is usually accomplished indirectly by variable-field and -temperature Mössbauer experiments, which afford D values with an estimated error of ~2 cm^{-1}. HFEPR, on the other hand, provides the possibility of measuring the zfs more directly and with much higher

---

[*] To whom correspondence should be addressed. E-mail: larryque@umn.edu (L.Q.); jtelser@roosevelt.edu (J.T.).

[†] Florida State University.

[‡] University of Minnesota.

[§] Roosevelt University.

(1) Solomon, E. I.; Brunold, T. C.; Davis, M. I.; Kemsley, J. N.; Lee, S.-K.; Lehnert, N.; Neese, F.; Skulan, A. J.; Yang, Y.-S.; Zhou, J. *Chem. Rev.* **2000**, *100*, 235–350.

(2) Costas, M.; Mehn, M. P.; Jensen, M. P.; Que, L., Jr *Chem. Rev.* **2004**, *104*, 939–986.

(3) Krebs, C.; Galonić Fujimori, D.; Walsh, C. T.; Bollinger, J. M. *Acc. Chem. Res.* **2007**, *40*, 484–492.

(4) Que, L., Jr *Acc. Chem. Res.* **2007**, *40*, 493–500.

(5) Shan, X.; Que, L., Jr *J. Inorg. Biochem.* **2006**, *100*, 421–433.

(6) Abbreviations: DFT, density functional theory; FDMRS, frequency domain magnetic resonance spectroscopy; HFEPR, high-frequency and -field electron paramagnetic resonance; HS, high spin; LS, low spin; **N4py**, bis(2-pyridylmethyl)bis(2-pyridyl)methylamine; TMC, tetramethylcyclam (1,4,8,11-tetramethyl-1,4,8,11-tetraazacyclotetradecane); TSR, two-state reactivity; zfs, zero-field splitting.

(7) Hirao, H.; Kumar, D.; Que, L., Jr.; Shaik, S. *J. Am. Chem. Soc.* **2006**, *128*, 8590–8606.

(8) Kaizer, J.; Klinker, E. J.; Oh, N. Y.; Rohde, J.-U.; Song, W. J.; Stubna, A.; Kim, J.; Münck, E.; Nam, W.; Que, L, Jr *J. Am. Chem. Soc.* **2004**, *126*, 472–473.

(9) Jensen, M. P.; Costas, M.; Ho, R. Y. N.; Kaizer, J.; Mairata i Payeras, A.; Münck, E.; Que, L, Jr.; Rohde, J.-U.; Stubna, A. *J. Am. Chem. Soc.* **2005**, *127*, 10512–10525.

(10) Schöneboom, J. C.; Neese, F.; Thiel, W. *J. Am. Chem. Soc.* **2005**, *127*, 5840–5853.

10.1021/ic800411c CCC: $40.75

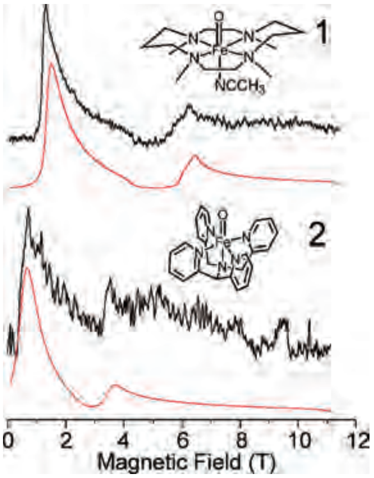

Figure 1. HFEPR spectra of **1** (upper black trace) with simulation (upper red trace) and **2** (lower black trace) with simulation (lower red trace). Experimental parameters: temperature, 4.2 K; frequency, 846 GHz (**1**), 676 GHz (**2**); field sweep rate, 5 T/min; optical modulation (chopping of a submillimeter wave beam, which yields an absorption line shape) at 500 Hz. Simulation parameters: $S = 1$; $D = +26.9$ cm^{-1}, $E = +0.095$ cm^{-1}, $g_{x,y} = 2.1$, $g_z = 2.04$ (**1**); $D = +22.05$ cm^{-1}, $E = 0$; $g_{\mathrm{iso}} = 2.01$ (**2**).

accuracy and precision. Over the past decade, HFEPR has been applied to a wide variety of transition-metal ion complexes with $S > 1/2$ and has determined their spin Hamiltonian parameters.[11,12] There has been success with HS Fe$^{\mathrm{II}}$ [13] and HS Fe$^{\mathrm{III}}$ centers[14] but thus far not with Fe$^{\mathrm{IV}}$. We report here the first successful application of HFEPR to the determination of the spin Hamiltonian parameters of two stable iron(IV) oxo complexes in the solid state: [FeO(TMC)(CH$_3$CN)](CF$_3$SO$_3$)$_2$ (**1**; see Figure 1 for structures)[15,16] and [FeO(**N4py**)](CF$_3$SO$_3$)$_2$ (**2**).[8]

Polycrystalline samples of **1** and **2** (typically 30–50 mg) were investigated by HFEPR at NHMFL using either the Millimeter and Submillimeter Wave Facility with a 25 T resistive magnet,[17] for which the frequency maximum has been recently extended to 900 GHz, or the EMR Facility with a 15/17 T superconducting magnet.[18]

Figure 1 (top) shows a representative HFEPR spectrum of **1** recorded at 4.2 K and 846 GHz. The spectrum exhibits two well-defined maxima, each corresponding to a major turning point within the powder pattern, at fields of 1.3 and 6.3 T, with weaker shoulders at ca. 3.7 and 5.7 T. At a lower frequency of ~810 GHz, these resonances collapse into a single zero-field transition. Below 800 GHz, a single feature is observed, which moves toward *higher* field with *decreasing* frequency. At 250 GHz, this signal broadens and weakens beyond recognition.

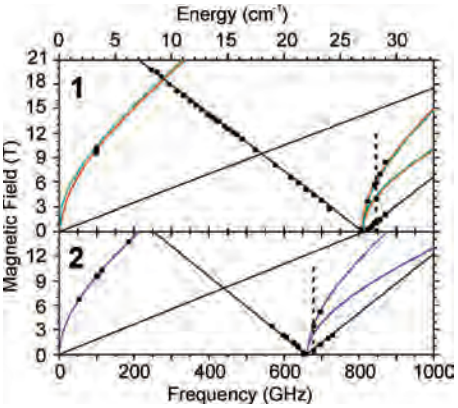

Figure 2. Plot of the resonant field position versus applied frequency (energy) for **1** (top) and **2** (bottom). Squares are experimental points. Black lines are calculated with the magnetic field parallel (||) to the molecular axis (z) and blue lines with the field perpendicular ($\perp \equiv x, y$): green for x; red for y. Simulation parameters are given in Table 1. The broken lines represent the frequency and field range of the spectra shown in Figure 1.

In accordance with our recently developed methodology of tunable-frequency HFEPR,[12] we plotted a full 2-D map of observed resonances as a function of the EPR frequency, which is shown in Figure 2 (top). This map is very characteristic of a spin triplet with highly axial, large-magnitude zfs, $D \sim 810$ GHz $= 27$ cm^{-1}.[19] To a high degree of certainty, it excludes the possibility of interpreting the EPR resonances in terms of a quintet state with the same D value because the perpendicular transitions have totally different field versus frequency behavior (see Figure S1 in the Supporting Information). A computer fit of the entire resonance data set provided a complete set of spin Hamiltonian parameters,[20] which are collected in Table 1 and compared with parameters deduced from Mössbauer data.[9]

Similar results were obtained for **2** at 4.2 K, as shown in Figure 1 (bottom), and its 2-D map of resonances is shown in Figure 2 (bottom). The outstanding feature is that the zero-field transition for **2** appears at significantly lower frequency (~660 GHz) than for **1**; however, the resonances originating from that transition could be followed only within a narrower frequency range (~560–730 GHz).

The HFEPR spectra of **1** and **2** show some significant differences at 15 K. A pair of weak resonances was observed near ~95 GHz and 10 T for **1**. In contrast, no such doubling was found for **2**, and an entire branch of resonances could be followed at 15 K over the frequency range of ~50–200 GHz. That no doubling of these resonances was observed means that the zfs tensor of **2** is effectively axial within the experimental line width (80–100 mT). The spin Hamiltonian parameters for **2** are also shown in Table 1. Data for a wide range of iron(IV) oxo systems are summarized in Table S1 in the Supporting Information. Note that for **1** we have

---

(11) Krzystek, J.; Ozarowski, A.; Telser, J. *Coord. Chem. Rev.* **2006**, *250*, 2308–2324.

(12) Krzystek, J.; Zvyagin, S. A.; Ozarowski, A.; Trofimenko, S.; Telser, J. *J. Magn. Reson.* **2006**, *178*, 174–183.

(13) Ozarowski, A.; Zvyagin, S. A.; Reiff, W. M.; Telser, J.; Brunel, L.-C.; Krzystek, J. *J. Am. Chem. Soc.* **2004**, *126*, 6574–6575.

(14) Miyajima, Y.; Yashiro, H.; Kashiwagi, T.; Hagiwara, M.; Hori, H. *J. Phys. Soc. Jpn.* **2004**, *73*, 280–286.

(15) Rohde, J.-U.; In, J.-H.; Lim, M. H.; Brennessel, W. W.; Bukowski, M. R.; Stubna, A.; Münck, E.; Nam, W.; Que, L., Jr *Science* **2003**, *299*, 1037–1039.

(16) Decker, A.; Rohde, J.-U.; Klinker, E. J.; Wong, S. D.; Que, L., Jr.; Solomon, E. I. *J. Am. Chem. Soc.* **2007**, *129*, 15983–15996.

(17) Zvyagin, S. A.; Krzystek, J.; van Loosdrecht, P. H. M.; Dhalenne, G.; Revcolevschi, A. *Physica B* **2004**, *346–347*, 1–5.

(18) Hassan, A. K.; Pardi, L. A.; Krzystek, J.; Sienkiewicz, A.; Goy, P.; Rohrer, M.; Brunel, L.-C. *J. Magn. Reson.* **2000**, *142*, 300–312.

(19) Desrochers, P. J.; Telser, J.; Zvyagin, S. A.; Ozarowski, A.; Krzystek, J.; Vicic, D. A. *Inorg. Chem.* **2006**, *45*, 8930–8941.

(20) A standard spin Hamiltonian was used to fit the data: $H = \beta_e \mathbf{g} \cdot S + D[S_z^2 - (1/3)S(S+1)] + E[S_x^2 - S_y^2]$.

Table 1. Spin Hamiltonian Parameters of Complexes **1** and **2**

complex	D (cm^{-1})	$\|E\|$ (cm^{-1})	$g_{x,y}$	g_z
$[Fe^{IV}O(TMC)(CH_3CN)]^{2+}$ (**1**)[a]	+26.95(5) *[28(2)]*[a]	0.070(35)	2.10(5)	2.04(1)
$[Fe^{IV}O(N4Py)]^{2+}$ (**2**)[a]	+22.05(5) *[24(2)]*[a]	0.000(25)	2.03(1)	1.95(5)

[a] Values in square brackets were obtained from Mössbauer analysis.[9]

confidence in the z component of the **g** tensor [2.04(1)], while its perpendicular components have 5-fold greater uncertainty, and the situation is reversed for **2**. This difference results from the number of resonances observed for particular branches, which, in turn, is related to systems' complicated spin-relaxation properties.

However, the zfs parameters are determined very accurately in both cases, and the rhombic parameter (E) is certainly nonzero for **1** while it is zero for **2**. It was also possible through simulations and thermodynamic considerations to confirm unequivocally the positive sign of D for both complexes. Thermal activation (observation at 15 K as opposed to 4.2 K) of perpendicular resonances appearing at low frequencies (<200 GHz), originating between the $M_S = |\pm1\rangle$ pair of levels, means that this pair of levels lies higher on the energy scale than the $M_S = |0\rangle$ level, which corresponds by convention to a positive D. An energy level diagram for **1** (ignoring slightly rhombic symmetry) is presented in Figure 3.

The spin Hamiltonian parameters directly determined here for **1** and **2** can be compared to those extracted from Mössbauer data.[9,15] The agreement is adequate for D (within 10%; see Table 1). One might assume that agreement between Mössbauer and HFEPR zfs data is a forgone conclusion. This is not necessarily the case. For another integer-spin iron complex, namely, HS Fe^{II} (d^6, $S = 2$) in a rubredoxin model, $(PPh_4)_2[Fe(SPh)_4]$, the agreement in zfs parameters between Mössbauer[21] and HFEPR[22] was quite poor (~30% difference in D). However, there was exact agreement between HFEPR and FDMRS spectroscopy, which directly measures zero-field transitions.[23,24] This discrepancy between Mössbauer and resonance methods may be due to the difficulty in fitting Mössbauer data for a highly rhombic system, which is the case for $[Fe(SPh)_4]^{2-}$ ($|E/D| = 0.24$).[22] Similar difficulties were obtained in analysis of magnetic susceptibility data for rhombic systems.[25] The agreement here between HFEPR and Mössbauer for **1** and **2** has important consequences. First, by extension, in all of these nearly axial iron(IV) oxo systems, the D values determined by Mössbauer are likely validated and can be confidently accepted to within ~10%. However, for more quantitative comparisons, HFEPR is needed to provide the necessary precision. This includes an accurate measurement of the rhombicity, which is relevant to optical studies[16] and, more importantly, of the g values, for which no meaningful values had been available. The g values are now in much better agreement with calculations[10] than was previously thought (see Table S1 in the Supporting Information).

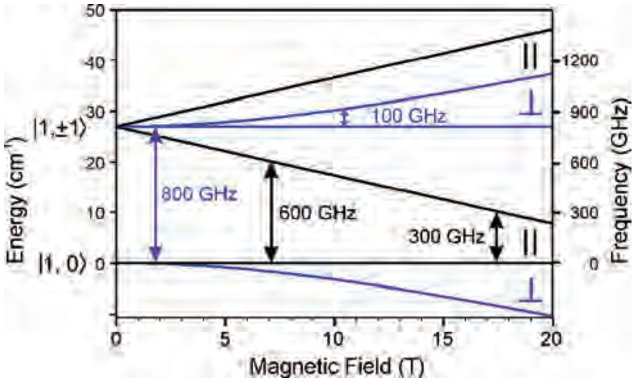

Figure 3. Energy level diagram for **1**. The zero-field $|S,M_S\rangle$ states are indicated at the left. The lines are generated using the parameters in Figure 1 but with $E = 0$ for clarity; black lines are with the magnetic field parallel (||) and blue lines perpendicular (⊥) to the molecular axis. The black arrows indicate the $|S,M_S\rangle = |1,0\rangle \rightarrow |1,\pm1\rangle$ parallel (z) transition, which is observed at numerous frequencies (shown here at 300 and 600 GHz), as indicated by points in Figure 2. The larger blue arrow indicates a perpendicular (xy) transition observable at only the highest frequencies (shown here at 800 GHz), as seen in Figure 1. The smaller blue arrow indicates a perpendicular transition observable at low frequencies (~100 GHz) and only at higher temperatures (15 K), as it corresponds to a transition from an excited M_S state that is relatively unpopulated at ~4 K.

This work thus shows that HFEPR is applicable to a further non-Kramers ion system, Fe^{IV}, opening possibilities for studies of related enzymes and of additional model complexes, such as those in which the axial ligand is varied.[26] The precise spin Hamiltonian parameters potentially obtainable on such complexes could serve as the basis for further computations, in particular to refine the TSR model.

Acknowledgment. This work has been supported by the NIH (Grant GM-33162, L.Q.) and by the NHMFL (IHRP; J.K. and J.T.), which is funded by NSF (Cooperative Agreement DMR 0654118), the State of Florida, and DOE. The 25 T magnet was funded by the W. M. Keck Foundation.

Supporting Information Available: A table of spin Hamiltonian parameters for iron(IV) oxo systems and a figure showing field versus frequency maps for hypothetical $S = 2$ states. This material is available free of charge via the Internet at http://pubs.acs.org.

IC800411C

---

(21) Petrouleas, V.; Simopoulos, A.; Kostikas, A.; Coucouvanis, D. *J. Phys., Colloq.* **1976**, *37*, C6–159–C6–164.

(22) Knapp, M. J.; Krzystek, J.; Brunel, L.-C.; Hendrickson, D. N. *Inorg. Chem.* **2000**, *39*, 281–288.

(23) Champion, P. M., Sievers, A. J. *J. Chem. Phys.* **1977**, *66*, 1819–1825. We use the term FDMRS for this type of far-IR spectroscopy.

(24) Mössbauer studies of $(PPh_4)_2[Fe(SPh)_4]$ were analyzed to give $D = 7.55$, $E = 1.69$ cm^{-1}.[21] FDMRS transitions were analyzed to give $D = 5.98$, $E = 1.42$ cm^{-1},[23] the values of which were later refined to give $D = 5.82(4)$, $E = 1.44(2)$ cm^{-1},[22] in agreement with those of HFEPR: $D = 5.84(2)$, $E = 1.42(1)$ cm^{-1}.[22]

(25) Krzystek, J.; Park, J.-H.; Meisel, M. W.; Hitchman, M. A.; Stratemeier, H.; Brunel, L.-C.; Telser, J. *Inorg. Chem.* **2002**, *41*, 4478–4487.

(26) Sastri, C. V.; Lee, J.; Oh, K.; Lee, Y. J.; Lee, J.; Jackson, T. A.; Ray, K.; Hirao, H.; Shin, W.; Halfen, J. A.; Kim, J.; Que, L., Jr.; Shaik, S.; Nam, W. *Proc. Natl. Acad. Sci. U.S.A.* **2007**, *104*, 19181–19186.